JB
Journals.ASM.org

# Succinyl-CoA:3-Sulfinopropionate CoA-Transferase from *Variovorax paradoxus* Strain TBEA6, a Novel Member of the Class III Coenzyme A (CoA)-Transferase Family

**Marc Schürmann,[a] Beatrice Hirsch,[a] Jan Hendrik Wübbeler,[a] Nadine Stöveken,[a] Alexander Steinbüchel[a,b]**

Institut für Molekulare Mikrobiologie und Biotechnologie, Westfälische Wilhelms-Universität Münster, Münster, Germany[a]; Environmental Sciences Department, King Abdulaziz University, Jeddah, Saudi Arabia[b]

**The *act* gene of *Variovorax paradoxus* TBEA6 encodes a succinyl-CoA:3-sulfinopropionate coenzyme A (CoA)-transferase, $Act_{TBEA6}$ (2.8.3.x), which catalyzes the activation of 3-sulfinopropionate (3SP), an intermediate during 3,3′-thiodipropionate (TDP) degradation. In a previous study, accumulation of 3SP was observed in a Tn*5*::*mob*-induced mutant defective in growth on TDP. In contrast to the wild type and all other obtained mutants, this mutant showed no growth when 3SP was applied as the sole source of carbon and energy. The transposon Tn*5*::*mob* was inserted in a gene showing high homology to class III CoA-transferases. In the present study, analyses of the translation product clearly allocated $Act_{TBEA6}$ to this protein family. The predicted secondary structure indicates the lack of a C-terminal α-helix. $Act_{TBEA6}$ was heterologously expressed in *Escherichia coli* Lemo21(DE3) and was then purified by Ni-nitrilotriacetic acid (NTA) affinity chromatography. Analytical size exclusion chromatography revealed a homodimeric structure with a molecular mass of 96 ± 3 kDa. Enzyme assays identified succinyl-CoA, itaconyl-CoA, and glutaryl-CoA as potential CoA donors and unequivocally verified the conversion of 3SP to 3SP-CoA. Kinetic studies revealed an apparent $V_{max}$ of 44.6 μmol $min^{-1}$ $mg^{-1}$ for succinyl-CoA, which corresponds to a turnover number of 36.0 $s^{-1}$ per subunit of $Act_{TBEA6}$. For 3SP, the apparent $V_{max}$ was determined as 46.8 μmol $min^{-1}$ $mg^{-1}$, which corresponds to a turnover number of 37.7 $s^{-1}$ per subunit of $Act_{TBEA6}$. The apparent $K_m$ values were 0.08 mM for succinyl-CoA and 5.9 mM for 3SP. Nonetheless, the *V. paradoxus* Δ*act* mutant did not reproduce the phenotype of the Tn*5*::*mob*-induced mutant. This defined deletion mutant was able to utilize TDP or 3SP as the sole carbon source, like the wild type. Complementation of the Tn*5*::*mob*-induced mutant with pBBR1MCS5::$acd_{DPN7}$ partially restored growth on 3SP, which indicated a polar effect of the Tn*5*::*mob* transposon on $acd_{TBEA6}$, located downstream of $act_{TBEA6}$.**

3,3′-thiodipropionate (TDP) is a nontoxic thioether and is widely used as an antioxidant in technical applications (1–4). Furthermore, it is used as a precursor substrate for the microbial production of polythioester (PTE) (5). With TDP in the presence of gluconate or fructose under nitrogen limitation, *Ralstonia eutropha* strain H16 accumulates heteropolymers consisting of 3-hydroxybutyrate (3HB) and 3-mercaptopropionate (3MP) (6). PTE homopolymers are synthesized by applying the artificial BPEC pathway in the recombinant *Escherichia coli* strain JM109(pBPP1) (7). Therefore, 3MP, 3-mercaptobutyrate (3MB), or 3-mercaptovalerate (3MV) is applied as a precursor substrate (7, 8). Only recently, the production of PTE homopolymers in *Advenella mimigardefordensis* $DPN7^T$ was achieved by applying 3,3′-dithiodipropionate (DTDP) (9, 10). Unfortunately, PTE homopolymer production by applying TDP is yet not possible. The availability of complete information about enzymes that are involved in TDP degradation would be beneficial to optimize PTE production.

*Variovorax paradoxus* is a Gram-negative, aerobic betaproteobacterium that belongs to the *Comamonadaceae* (11, 12). This microorganism could often be isolated from the rhizosphere of cereals (13–16), and growth on carbohydrates like glucose, mannose, or galactose is frequently observed (12). Additionally, strains of *V. paradoxus* are able to utilize widespread, xenobiotic compounds like 2,4-dichlorophenoxyacetic acid (17) or 2,4-dinitrotoluene (18). *V. paradoxus* strain TBEA6 was isolated due to its ability to degrade TDP and use it as the sole source of carbon and energy (19).

In a previous study, a putative degradation pathway for TDP was postulated based on Tn*5*::*mob* mutagenesis with *V. paradoxus* strain TBEA6 and analysis of the obtained mutants (19) (Fig. 1). Accumulation of the supposed degradation intermediate 3-sulfinopropionate (3SP) was observed during cultivation of one of the resulting Tn*5*::*mob*-induced mutants (mutant 1/1) in mineral salt medium (MSM) containing TDP. In contrast to the wild type, mutant 1/1 was unable to utilize 3SP as the sole source of carbon and energy for growth (19). The insertion of Tn*5*::*mob* in this mutant was detected in a gene putatively coding for an acyl coenzyme A (CoA)-transferase ($Act_{TBEA6}$). Reverse transcription (RT)-PCR analyses of RNA from the wild type revealed constitutive transcription of this gene, irrespective of whether TDP or succinate was present as the sole source of carbon and energy (19). CoA-transferases catalyze the reversible transfer reaction of CoA from a donor to a free acid by formation of a CoA thioester (20, 21). Therefore, it was expected that the translational product catalyzes the activation of 3SP to its corresponding CoA ester.

CoA-transferases are classified by sequence similarities and re-

Received 22 April 2013 Accepted 10 June 2013
Published ahead of print 14 June 2013
Address correspondence to Alexander Steinbüchel, steinbu@uni-muenster.de.
Supplemental material for this article may be found at http://dx.doi.org/10.1128/JB.00456-13.

doi:10.1128/JB.00456-13

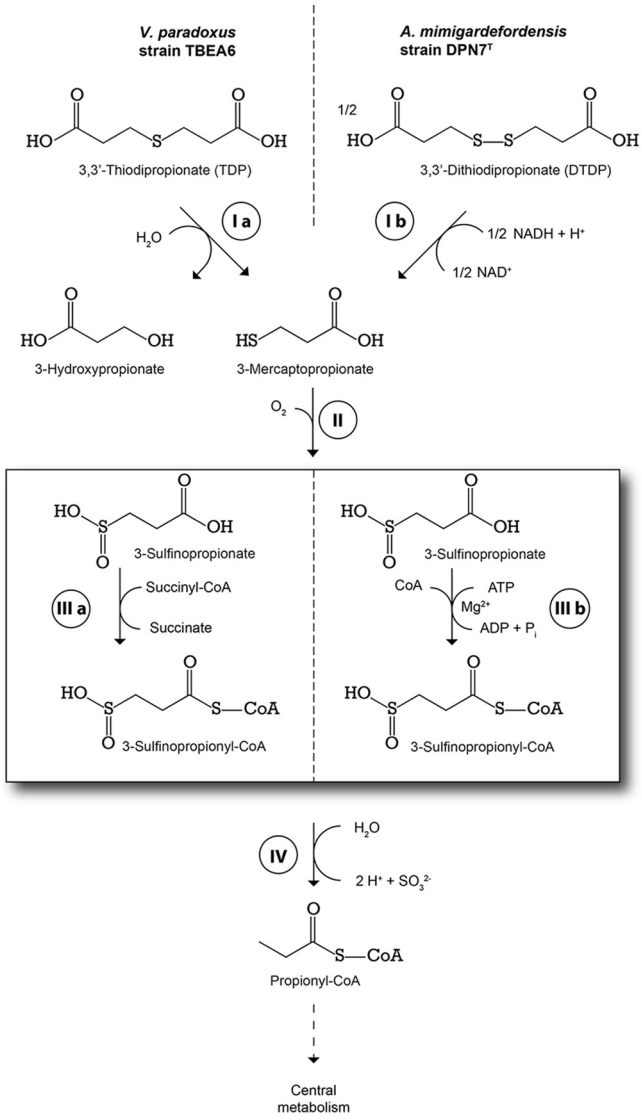


**FIG 1** Putative degradation pathways of 3,3′-thiodipropionate (TDP) in *V. paradoxus* strain TBEA6 and of 3,3′-dithiodipropionate (DTDP) in *A. mimigardefordensis* strain DPN7$^T$. Bruland et al. (19) postulated that in *V. paradoxus* strain TBEA6, the organosulfur compound TDP is initially cleaved to 3-hydroxypropionate (3HP) and 3-mercaptopropionate (3MP), putatively by a flavin adenine dinucleotide (FAD)-dependent oxidoreductase (step I a). In *A. mimigardefordensis* strain DPN7$^T$, a dihydrolipoamide dehydrogenase (LpdA) catalyzes the initial cleavage of DTDP (step I b), yielding two molecules of 3MP (62). In both bacteria, 3MP is further oxygenated to 3-sulfinopropionate (3SP) by a 3MP-dioxygenase (step II) (19). The acyl-CoA-transferase ($Act_{TBEA6}$) investigated in this study can catalyze the transformation of 3SP to the corresponding CoA thioester, 3SP-CoA (step III a). In *A. mimigardefordensis* DPN7$^T$, 3SP is activated by $SucCD_{DPN7}$, a succinate-CoA ligase, to 3SP-CoA (step III b) (37). Subsequent abstraction of the sulfur moiety is catalyzed by a desulfinase, Acd, yielding sulfite and propionyl-CoA (step IV) (51). The latter enters the central metabolism via the methylcitric acid cycle.

action mechanisms into three families (21). In the first family, both substrates (CoA donor and CoA acceptor) are not bound to the enzyme simultaneously, but two consecutive enzyme-substrate complexes are formed. Hence, this mechanism is also known as the "ping-pong" mechanism (21, 22). The formation of a covalent CoA thioester intermediate with an active-site glutamate residue is characteristic for members of this family.

The CoA-transferases of the second family are part of a citrate lyase (EC 2.8.3.10) or citramalate lyase (EC 2.8.3.11) complex that consists of three subunits (23). The CoA-transferase catalyzes the exchange of free citrate or citramalate against the acetyl-thioester group of an acyl carrier protein (ACP). During this reaction, both substrates (citrate/citramalate and the acetyl-thioester) are not covalently attached to the transferase, and a ternary complex is built (21, 23–25).

Members of family III differ significantly in sequences and reaction mechanisms. They are often involved in unusual biochemical pathways in anaerobic bacteria and activate organic acids for further reactions, such as decarboxylation, β-oxidation, or elimination of α/β-hydroxyl groups (21). Their primary structures showed only few conserved amino acids, which makes it difficult to predict the structural conservation within this family (26). Nonetheless, the crystal structures of several representatives have been elucidated (20, 26–30). They indicate that family III CoA-transferases appear as intertwined dimers in which each monomer forms a ring with a hole in the center through which the other monomer is threaded (29). The mechanism proceeds via the formation of anhydrides between a highly conserved aspartate residue (Asp169 with respect to crotonobetainyl-CoA:carnitine CoA-transferase [CaiB] from *E. coli*) in the active site and the substrates. Crystal structure analysis and kinetic experiments indicate that the reaction is completed prior to the release of any product (20). Consequently, two different mechanisms were discovered, which close the active site during catalysis. In the first mechanism, a glycine-rich loop takes different conformations as described for formyl CoA-transferase (20, 26–28, 31). For CaiB from *Escherichia coli*, a representative of the second mechanism, the binding of the CoA triggers a domain shift that leads to the closure of the active site (30).

This study reports on the enzymatic activation of 3SP, an organosulfur compound, to the corresponding CoA thioester and the biochemical characterization of $Act_{TBEA6}$ as a novel member of class III CoA-transferases.

## MATERIALS AND METHODS

**Bacterial strains and cultivation conditions.** All strains used in this study are listed in Table 1. Cells of *V. paradoxus* were cultivated at 30°C on solid MSM (32) containing 20 mM gluconate, 20 mM TDP, or 20 mM 3SP as the sole source of carbon and energy to test carbon source utilization. Cells of *E. coli* were cultivated in lysogeny broth (LB) medium at 37°C under the same conditions (33). Carbon sources were supplied as filter-sterilized stock solutions as indicated in the text. For maintenance of plasmids, antibiotics were prepared according to the method of Sambrook et al. (33) and added to the media at the following concentrations: ampicillin, 75 μg/ml; kanamycin, 50 μg/ml; gentamicin, 20 μg/ml; and tetracycline, 12.5 μg/ml. In *E. coli*, heterologous expression of genes under the control of a *lac* promoter was achieved by cultivation in ZYP-5052 medium, an autoinductive medium, according to Studier et al. (34) or by induction with 0.4 mM IPTG (isopropyl-β-D-thiogalactopyranoside) in LB medium.

**Chemicals.** TDP of high-purity grade was purchased from Sigma-Aldrich (Steinheim, Germany). 3-Sulfinopropionate was synthesized according to Jollès-Bergeret (35); the procedure was modified by one repetition of the step for alkaline cleavage of the intermediate *bis*-(2-carboxyethyl)sulfone (36). The synthesis and purity of the substance were confirmed by gas chromatography-mass spectrometry (GC-MS) as described elsewhere (37) and were at least 95.0%. Acetic anhydride, propionic anhydride, butyric anhydride, valeric anhydride, isobutyric anhydride, isovaleric anhydride, maleic anhydride, crotonic anhy-

**TABLE 1** Strains and plasmids used in this study

| Strain or plasmid | Description or sequence (5′→3′)[a] | Source or reference |
|---|---|---|
| Strains | | |
| *V. paradoxus* | | |
| TBEA6 | Wild type, TDP and 3SP utilizing | 19 |
| TBEA6 mutant 1/1 | Tn*5*::*mob*-induced mutant, retarded growth on TDP, 3SP-negative, $Km^r$ | 19 |
| TBEA6 mutant 1/1(pBBR1MCS-5::$acd_{DPN7}$) | TDP negative, partially restored growth on 3SP | This study |
| TBEA6 Δ$act_{TBEA6}$ | Precise deletion mutant of *V. paradoxus* TBEA6, lacks $act_{TBEA6}$ | This study |
| EPS | Wild type, whole genome sequence available, TDP and 3SP negative | 53 |
| B4 | Wild type, mercaptosuccinic acid utilizing, TDP and 3SP negative | 60 |
| S110 | Wild type, first genome sequenced from genus *Variovorax*, TDP and 3SP negative | 61 |
| *E. coli* | | |
| One Shot Mach1-$T1^R$ | $F^-$ ϕ80*lacZ*ΔM15 Δ*lacX74 hsdR*($r_K^-$ $m_K^+$) Δ*recA1398 endA1 tonA* | Invitrogen, Carlsbad, CA |
| Top10 | $F^-$ *mczA* Δ(*mrr-hsdRMS-mcrBC*) *rpsL nupG* ϕ80*lacZ*ΔM15 Δ*lacX74 deoR recA1 araD139* Δ(*ara-leu*)*7697 galU galK endA1* | Invitrogen, Carlsbad, CA |
| Lemo21(DE3) | *fhuA2* [*lon*] *ompT gal* (λ DE3) [*dcm*] Δ*hsdS*/pLemo($Cam^r$) λ DE3 = λ sBamHIo ΔEcoRI-B *int*::(*lacI*::*PlacUV5*::T7 gene 1) *i21* Δ*nin5* pLemo = pACYC184-*PrhaBAD-lysY* | New England Biolabs, Inc. |
| Plasmids | | |
| pCR2.1-TOPO | $Km^r$ $Ap^r$ *lacZ*α | Invitrogen, Carlsbad, CA |
| pCR2.1-TOPO::$act_{TBEA6}$ | $Km^r$ $Ap^r$ *lacZ*α $act_{TBEA6}$ | This study |
| pET22b(+) | $Ap^r$, N-terminal *pelB*-leader sequence for potential excretion to cytoplasm, C-terminal $His_6$ tag | Novagen, Madison, WI |
| pET22b(+)::$act_{TBEA6}$ | $Ap^r$, $act_{TBEA6}$, expressing *pelB*-$Act_{TBEA6}$-$His_6$ | This study |
| pJQ200mp18Tc | *sacB oriV oriT traJ* $Tc^r$ | 47–49 |
| pJQ200mp18Tc::Δ$act_{TBEA6}$ | *sacB oriV oriT traJ* $Tc^r$, 526-bp upstream and 691-bp downstream flanks of $act_{TBEA6}$ ligated with NdeI (1,223 bp) | This study |
| pBBR1MCS-5 | Broad-host-range cloning vector, $Gm^r$ *lacZ*α | 52 |
| pBBR1MCS-5::$acd_{DPN7}$ | pBBR1MCS-5 containing *acd* gene of *A. mimigardefordensis* $DPN7^T$ and 14-bp upstream region as 1,220-bp ApaI-PstI fragment, $Gm^r$ | 51 |

[a] For abbreviations used in the genotypes of *E. coli*, see reference 67. $Ap^r$, ampicillin resistance; $Km^r$, kanamycin resistance; $Tc^r$, tetracycline resistance; $Gm^r$, gentamicin resistance.

dride, succinic anhydride, itaconic anhydride, and glutaric anhydride were purchased from Sigma-Aldrich (Steinheim, Germany). Thiodiglycolic anhydride for synthesis of 3-thiaglutaryl-CoA was purchased from Alfa Aesar (Karlsruhe, Germany). Mercaptosuccinic acid was purchased from Acros Organics (Geel, Belgium).

Acetyl-CoA was purchased from Sigma-Aldrich (Steinheim, Germany) or synthesized according to the method of Simon and Shemin (38). For synthesis of propionyl-CoA, butyryl-CoA, valeryl-CoA, isobutyryl-CoA, isovaleryl-CoA, crotonyl-CoA, maleyl-CoA, succinyl-CoA, itaconyl-CoA, glutaryl-CoA, or 3-thiaglutaryl-CoA, according to the method of Simon and Shemin (38), 10 mg of the trilithium salt of coenzyme A (Merck KGaA, Darmstadt, Germany) was dissolved in 0.5 M $K_2CO_3$ or Tris-HCl (pH 8.0). The solution was stirred on ice, and small portions of the respective anhydride were added to this solution until no free coenzyme A was detectable by Ellman′s spot test (39). The pH value of the solution was then adjusted to 4.5 by addition of concentrated phosphoric acid or 9 M hydrochloric acid. The resulting acyl-CoA thioesters were immediately applied for enzyme assays or stored at −20°C.

**Isolation and manipulation of DNA.** Chromosomal DNA of *V. paradoxus* strain TBEA6 was isolated according to the method of Marmur (40). Plasmid DNA was isolated from *E. coli* using the peqGOLD plasmid miniprep kit I from PEQLAB Biotechnologie GmbH (Erlangen, Germany) according to the manufacturer's manual. DNA was digested with restriction endonucleases under the conditions described by the manufacturer. PCRs were carried out in an Omnigene HBTR3CM DNA thermal cycler (Hybaid, Heidelberg, Germany) using Platinum *Taq* DNA polymerase (Invitrogen, Carlsbad, CA). PCR products were isolated from an agarose gel and purified using the NucleoTrap kit (Macherey and Nagel, Düren, Germany) according to the manufacturer's instructions. T4 DNA ligase was purchased from Invitrogen (Carlsbad, CA). The primers were synthesized by MWG-Biotech AG (Ebersberg, Germany) and are listed in Table S1 in the supplemental material.

**Transfer of DNA.** Competent cells of *E. coli* strains were prepared and transformed by the $CaCl_2$ procedure (33).

**DNA sequencing and sequence data analysis.** DNA sequencing was performed by Seqlab (Göttingen, Germany) or by the Institut für Klinische Chemie und Laboratoriumsmedizin at the Universitätsklinikum Münster (Germany). The latter sequenced the samples according to the method of Sanger et al. (41) by applying the BigDye Terminator v3.1 cycle sequencing kit according to the manufacturer's manual (Applied Biosystems, Darmstadt, Germany). Samples were submitted to the Institut für Klinische Chemie und Laboratoriumsmedizin for purification of the extension products and sequencing in an ABI Prism 3700 DNA analyzer (Applied Biosystems, Darmstadt, Germany). Sequences were analyzed using the program BLAST (National Center for Biotechnology Information; http://www.ncbi.nlm.nih.gov/BLAST/) (42). The program BioEdit (43) was used for multiple sequence alignments. Secondary structure predictions were performed using the Jpred3 server (44) with Jnet version 2.2 and UniRef90 release 15.4. Predictions of molecular mass and the extinction coefficient of heterologously expressed $Act_{TBEA6}$ were performed using Expasy Protparam (45).

**Elucidation of the upstream and downstream region of the *act-acd-bug* cluster.** A PCR-based two-step genome-walking method (46) was used to sequence the upstream and downstream region adjacent to the known *act-acd-bug* cluster. Walking and sequencing primers were constructed as described by Pilhofer et al. (46) and are listed in Table S1 in the supplemental material. Genomic DNA of the wild type was isolated according to Marmur (40). Starting from the known sequence of $act_{TBEA6}$ (19), the upstream region was amplified with three walking steps (walking primers 1 to 3). The amplification products were sequenced with primers ActSeq1, ActSeq2, and ActSeq6 in the forward (upstream) direction. For validation of the obtained sequence, the sequencing primers ActSeq3rev, ActSeq4rev, and ActSeq5rev with a reverse orientation were used. As reported previously (19), the sequence of *bug* (*Bordetella* uptake gene), cod-

ing for an extracytoplasmatic solute receptor downstream of $act_{TBEA6}$, was incomplete. Hence, another walking step starting from the known sequence of *bug* applied the primers ActWalk5 and ActSeq7 and revealed the missing sequence information of *bug*.

**Cloning of $Act_{TBEA6}$.** $act_{TBEA6}$ was amplified from total genomic DNA of *V. paradoxus* strain TBEA6 by PCR using Platinum *Taq* DNA polymerase (Invitrogen, Karlsruhe, Germany) and the following oligonucleotides: *act_Hind*III_For and *act_Xho*I_Rev_oS (see Table S1 in the supplemental material). PCR products were isolated from agarose gels using the peqGOLD GelExtraction Kit (PEQLAB Biotechnologie GmbH, Erlangen, Germany) and ligated with pCR2.1-TOPO DNA (Invitrogen, Carlsbad, CA). Ligation products were used for transformation of $CaCl_2$ competent cells of *E. coli* OneShot Mach1-$T1^R$, and transformants were selected on LB agar plates containing IPTG and X-Gal (5-bromo-4-chloro-3-indolyl-β-D-galactopyranoside) plus ampicillin. For heterologous expression in the T7 promoter/polymerase-based expression vector pET22b(+) (Novagen, Madison, WI), $act_{TBEA6}$ was obtained by digestion of hybrid plasmid pCR2.1-TOPO::$act_{TBEA6}$ with restriction endonucleases HindIII and XhoI and purified from an agarose gel using the peqGOLD GelExtraction kit (PEQLAB Biotechnologie GmbH, Erlangen, Germany). After ligation with the expression vector pET22b(+), which was linearized with the same restriction endonucleases, the ligation product, pET22b(+)::$act_{TBEA6}$ (see Fig. S1 in the supplemental material), was used for transformation of $CaCl_2$-competent cells of *E. coli* Top10. After selection of transformants using LB medium containing ampicillin, the hybrid plasmids were isolated, analyzed by sequencing, and used for transformation of $CaCl_2$-competent cells of *E. coli* Lemo21(DE3) (New England BioLabs, Inc., Ipswich, MA).

**Construction of an *act* precise deletion gene replacement plasmid.** The 526- and 691-bp fragments upstream and downstream of $act_{TBEA6}$ were amplified by using the primers *Xba*I_upAct/*Nde*I_upAct or *Nde*I_downAct/*Xba*I_downAct, respectively. The oligonucleotides used for PCR are listed in Table S1 in the supplemental material. The resulting fragments were NdeI digested and ligated to yield a 1,223-bp fragment. This fragment was amplified using *Xba*I_upAct/*Xba*I_downAct, and the resulting PCR product was cloned into the XbaI site of pJQ200mp18Tc (47–49) to yield pJQ200mp18Tc::Δ*act*.

**Construction of an *act* gene deletion strain using the *sacB* system.** Standard protocols were adapted to accomplish gene replacement in strain *V. paradoxus* (47–49). Plasmid pJQ200mp18Tc::Δ$act_{TBEA6}$ was used to generate the *V. paradoxus* Δ$act_{TBEA6}$ mutant. The plasmid was mobilized from *E. coli* donor strain S17-1 to the *V. paradoxus* TBEA6 recipient strain by the spot agar mating technique (50). Positive transconjugants were screened on MSM containing 50 mM gluconate plus tetracycline. After cultivation in liquid nutrient broth for 20 h, samples were transferred to solid NB medium containing saccharose (10% [wt/vol]). Growing strains had lost the suicide plasmid. A successfully generated gene replacement strain was identified and confirmed by PCR analyses and DNA sequencing using the oligonucleotides listed in Table S1 in the supplemental material. Oligonucleotides up_*act*_proof and down_*act*_proof served to verify that $act_{TBEA6}$ was deleted in the *act-acd-bug* cluster. Oligonucleotides *act*_int_fwd and *act*_int_rev were used to verify that $act_{TBEA6}$ was not incorporated at a different position in the genome.

**Construction of *V. paradoxus* TBEA6 1/1(pBBR1MCS-5::$acd_{DPN7}$).** The complementation vector pBBR1MCS-5::$acd_{DPN7}$ was constructed and described in a previous study (51, 52). In this study, the vector was first transferred to $CaCl_2$-competent cells of *E. coli* S17-1. Vector-harboring clones were screened on LB agar plates containing gentamicin. The vector was then transferred to *V. paradoxus* TBEA6 1/1 by conjugation (48).

**Preparation of crude extracts.** Cells from 50- to 100-ml cultures were harvested by centrifugation (15 to 45 min, 4°C, 3,400 × *g*), washed twice with sterile saline, and resuspended in the appropriate buffers. For purification of histidine-tagged fusion proteins, the buffers were prepared as recommended by the manufacturer of the His Spin Trap affinity columns (GE Healthcare, Uppsala, Sweden). Cells were resuspended in 50 mM sodium phosphate binding buffer or 50 mM Tris-HCl buffer (both pH 7.4), containing 500 mM sodium chloride and 20 mM imidazole and afterwards disrupted by a 3-fold passage through a French press ($100 \times 10^6$ Pa). Soluble protein fractions of crude extracts were obtained in the supernatants after 1 h of centrifugation at 100,000 × *g* and 4°C and were used for enzyme purifications. Protein concentrations were determined as described by Bradford (53) or by applying a NanoDrop 2000 spectrophotometer (Fisher Scientific, Schwerte, Germany) and the calculated extinction coefficient of (51.590 $mM^{-1}$ $cm^{-1}$) at 280 nm.

**IMAC.** Immobilized metal-chelate affinity chromatography (IMAC) was performed as follows. To obtain purified histidine-tagged fusion proteins, His Spin Trap affinity columns (GE Healthcare, Uppsala, Sweden) were used according to the manufacturer's instructions. Ni-nitrilotriacetic acid (NTA) columns were equilibrated with 20 mM sodium phosphate buffer (pH 7.4), containing 20 mM imidazole and 500 mM sodium chloride. The same buffer containing 40 mM imidazole was used for the washing step, while the elution buffer contained 500 mM imidazole.

**Analytical SEC.** The molecular mass of $Act_{TBEA6}$ was determined by analytical size exclusion chromatography (SEC) using a Superdex 200 HR column. The column was equilibrated with 50 mM sodium phosphate buffer (pH 7.5), containing 150 mM sodium chloride. Calibration was performed applying chymotrypsinogen A (25 kDa), ovalbumin (44 kDa), conalbumin (75 kDa), aldolase (158 kDa), ferritin (440 kDa), and blue dextran 2000 (GE Healthcare, Uppsala, Sweden) according to the manufacturer's instructions. For each determination, 300 μg of purified heterologous $Act_{TBEA6}$ was applied to the column. The column was operated at a flow rate of 0.750 ml/min.

**Enzyme assays. (i) Initial identification of an appropriate CoA donor for $Act_{TBEA6}$.** The heterologously expressed $Act_{TBEA6}$ was assayed by incubating 20 μg/ml purified enzyme in 50 mM sodium phosphate buffer (pH 7.4) for 1 h at 30°C in the presence of 5 mM 3SP and 5 mM acetyl-CoA, propionyl-CoA, butyryl-CoA, crotonyl-CoA, or succinyl-CoA, respectively. The reaction was stopped by addition of 50 μl (10% [wt/vol]) trifluoroacetic acid (TFA). The samples were analyzed by high-pressure liquid chromatography (HPLC)-electrospray ionization (ESI) MS for the formation of 3SP-CoA. Samples with heat-inactivated protein (15 min at 95°C) and soluble protein fractions from cells harboring only the expression vector without $act_{TBEA6}$ (vector control) served as a control, or one of the substrates was omitted at a time.

**(ii) Determination of kinetic parameters.** 3SP-CoA formation by $Act_{TBEA6}$ was measured by applying *A. mimigardefordensis* strain $DPN7^T$ 3SP-CoA desulfinase ($Acd_{DPN7}$) as a coupling enzyme in an aerobic continuous spectrophotometric assay (51). Kinetic parameters were determined in cuvettes with a total volume of 1 ml containing 50 mM Tris-HCl (pH 7.6), 150 mM NaCl, 0.2 mM 5,5′-dithiobis(2-nitrobenzoic acid) (DTNB), and purified $Acd_{DPN7}$ as an auxiliary enzyme. Different amounts of $Acd_{DPN7}$ were tested to ensure that the auxiliary enzyme was not rate limiting. After preincubation for 2.5 min at 30°C, the reaction was started by addition of purified recombinant $Act_{TBEA6}$ (0.5 μg). The increase in absorption was measured at 412 nm ($\varepsilon = 14.150$ $mM^{-1}$ $cm^{-1}$) and corrected for the observed increase in absorbance based on the nonenzymatic decomposition of succinyl-CoA at pH 7.6. Activity was measured for 10 different concentrations of succinyl-CoA ranging from 0.0 mM to 1.0 mM (with a constant concentration of 10 mM 3SP) or for 12 concentrations of 3SP ranging from 0 to 100 mM (with a constant concentration of 0.2 mM succinyl-CoA). All measurements were done in triplicate at 30°C. The apparent $V_{max}$ and $K_m$ were determined by fitting the obtained data to the Michaelis-Menten equation.

**(iii) Utilization of CoA donors other than succinyl-CoA.** The assay mixture contained 0.2 mM DTNB, 10 mM 3SP, and an excess of $Acd_{DPN7}$ in 50 mM Tris-HCl (pH 7.6)–150 mM NaCl in a final volume of 1 ml. After preincubation for 1.5 min at 30°C, one of the following CoA esters was added to a final concentration of 0.13 mM: acetyl-CoA, propionyl-CoA, butyryl-CoA, valeryl-CoA, isobutyryl-CoA, isovaleryl-CoA, croto-

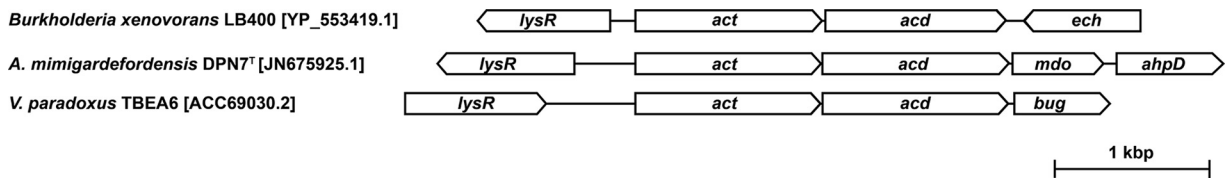


**FIG 2** Gene organization in proximity of *act* orthologues in *V. paradoxus* strain TBEA6 and other bacteria. *lysR*, transcription factor; *act*, acyl-CoA-transferase; *acd*, acyl-CoA dehydrogenase; *ech*, enoyl-CoA hydratase/isomerase; *mdo*, 3-mercaptopropionate dioxygenase; *ahpd*, alkylhydroperoxidase; *bug*, *Bordetella* uptake gene.

nyl-CoA, maleyl-CoA, succinyl-CoA, itaconyl-CoA, glutaryl-CoA, and 3-thiaglutaryl-CoA. After incubation for another minute, the reaction was started by addition of 42 μg of purified recombinant $Act_{TBEA6}$. The increase in absorbance was monitored at 412 nm.

**(iv) Utilization of CoA acceptors other than 3SP.** The assay mixture with a final volume of 1 ml in 50 mM Tris-HCl (pH 7.6)–150 mM NaCl contained 0.1 mM succinyl-CoA, 10 μg purified heterologous $Act_{TBEA6}$, and 5 mM each of the following putative CoA acceptors: sodium acetate, sodium propionate, itaconic acid, sodium fumarate, mercaptosuccinic acid, or sodium glutarate. Stock solutions of the corresponding substrates were adjusted to a pH range of 7.0 to 8.0 in advance. After 15 min of incubation at 30°C, the reaction was stopped by addition of 30 μl (15% [wt/vol]) trichloroacetic acid. Samples were analyzed for formation of the corresponding CoA esters by HPLC-ESI-MS.

**Inactivation experiments.** Hydroxylamine and sodium borohydride were applied in two inactivation experiments.

**(i) Inactivation by hydroxylamine.** A total of 210 μg purified recombinant $Act_{TBEA6}$ was incubated for 10 min at 30°C in 490 μl 50 mM Tris-HCl (pH 7.6), with 150 mM NaCl, either containing or lacking succinyl-CoA (2 mM). Subsequently, 5 μl 1 M hydroxylamine solution (in $H_2O$ [pH 7.0], adjusted with 5 M NaOH) was added to a final concentration of 10 mM, and the reaction mixture was incubated for an additional 10 min at 30°C. Afterwards, the reaction mixture was diluted 1:10 with 50 mM Tris-HCl (pH 7.6)–150 mM NaCl and stored on ice until enzyme activity was determined with the coupled spectrophotometric assay. Activity was measured in triplicate for the enzyme solutions incubated with or without succinyl-CoA.

**(ii) Inactivation by sodium borohydride.** A total of 210 μg purified recombinant $Act_{TBEA6}$ (from the same batch mentioned above) was incubated for 10 min at 30°C in 490 μl 500 mM Tris-HCl (pH 7.6), either containing or lacking succinyl-CoA (2 mM). Subsequently, 5 μl 1 M sodium borohydride in 1 M NaOH was added, followed by addition of 5 μl 1 M HCl immediately afterwards. The reaction mixture was incubated for an additional 10 min at 30°C. Afterwards, the reaction mixture was diluted 1:10 with 50 mM Tris-HCl (pH 7.6)–150 mM NaCl and stored on ice until enzyme activity was determined with the coupled spectrophotometric assay. Activity was measured in triplicate for the enzyme solutions incubated with or without succinyl-CoA.

**Analysis of CoA ester formation by HPLC-ESI MS.** Formation of 3SP-CoA during enzyme assays was followed by high-pressure liquid chromatography in combination with electrospray ionization mass spectrometry (HPLC-ESI MS) based on a method described earlier (37). Analyses were carried out using an UltiMate 3000 HPLC apparatus (Dionex GmbH, Idstein, Germany) connected directly to an LXQ Finnigan (ThermoScientific, Dreieich, Germany) mass spectrometer. An Acclaim 120 $C_{18}$ reversed-phase LC column (4.6 by 250 mm, 5 μm, 120-Å pores; Dionex GmbH, Idstein, Germany) served to separate the CoA esters at 30°C. A gradient system was used, with 50 mM ammonium acetate (pH 5.0) adjusted with acetic acid (A) and 100% (vol/vol) methanol (B) as eluents. Elution occurred at a flow rate of 0.3 ml/min. Ramping was performed as follows: equilibration with 90% eluent A for 2 min before injection and afterwards a change from 90% to 45% eluent A in 20 min, followed by holding for 2 min and then returning to 90% eluent A within 5 min. Detection of CoA esters occurred at 259 nm by a photodiode array detector. The instrument was tuned by direct infusion of a solution of 0.4 mM CoA at a flow rate of 10 μl/min into the ion source of the mass spectrometer to optimize the ESI MS system for maximum generation of protonated molecular ions (parents) of CoA derivatives. The following tuning parameters were retained for optimum detection of CoA esters: capillary temperature, 300°C; sheet gas flow, 12 liters/h; auxiliary gas flow, 6 liters/h; sweep gas flow, 1 liter/h. The mass range was set to *m/z* 50 to 1,000 Da when run in the scan mode. The collision energy in the MS-MS mode was set to 30 V and delivered fragmentation patterns that are in good accordance with those found in other publications (54).

**Nucleotide sequence accession numbers.** The DNA sequence and the deduced amino acid sequence of the gene cluster harboring $act_{TBEA6}$ were deposited in the GenBank database under accession no. EU449952.3. The accession no. for $act_{TBEA6}$ is ACC69030.2. DNA sequences for Act from *V. paradoxus* strain B4 and *A. mimigardefordensis* strain DPN7$^T$ are available under accession no. JN675924.1 ($act_{B4}$) and JN675925.1 ($act_{DPN7}$), respectively.

## RESULTS

**Gene organization.** In this study, the sequence of the regions adjacent to *act* was revealed by applying the genome-walking method as described in Materials and Methods (Fig. 2). The new sequence information was deposited as an update of EU49952 in the GenBank database.

The gene organization in proximity to $act_{TBEA6}$ resembles the gene organization found in *A. mimigardefordensis* DPN7$^T$ and *Burkholderia xenovorans* LB400, which harbor *act* genes coding for 76% and 57% identical amino acids, respectively, in comparison to $act_{TBEA6}$. In all strains, *lysR*, most likely coding for a LysR-type transcriptional regulator, is located upstream of *act* (Fig. 2), and a gene showing homology to acyl-CoA dehydrogenases (*acd*) is found in the downstream region. Only recently it was shown that $acd_{DPN7}$ encodes a 3SP-CoA desulfinase (51). $Acd_{TBEA6}$ shows high homology to $Acd_{DPN7}$ (79% identical and 88% similar amino acid residues) and to $Acd_{LB400}$ (64% identical and 76% similar residues).

Genes with high similarity to $act_{TBEA6}$ were searched within the available genome sequences of *V. paradoxus* strains EPS, S110, and B4 to investigate if this gene cluster is generally present in strains of *V. paradoxus*. Homologs (*V. paradoxus* EPS, YP_004152464.1; *V. paradoxus* S110, YP_002942048.1; *V. paradoxus* B4, JN675924.1) showed 49% identical amino acids in comparison to $act_{TBEA6}$. Although a gene coding for a putative acyl-CoA dehydrogenase was found in the upstream region, comparison of its sequence to that of the $acd_{DPN7}$ gene indicates that amino acid residues putatively characteristic for 3SP-CoA desulfinases (R84, C122, and Q246 according to $Acd_{DPN7}$ numbering) (data not shown) (51) are absent. Hence, these *acd* genes are most probably not coding for 3SP-CoA desulfinases.

**Utilization of TDP or 3SP by different strains of *V. paradoxus*.** *V. paradoxus* strains TBEA6, EPS, S110, and B4 were cul-

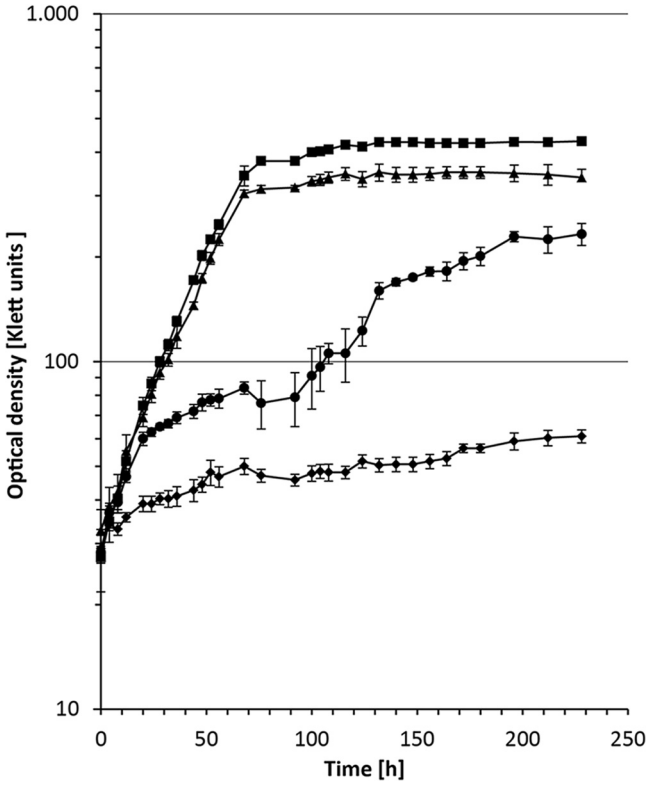


**FIG 3** Growth on 3-sulfinopropionate (3SP). Cells of the wild-type *V. paradoxus* strain TBEA6, the *V. paradoxus* TBEA6 Δ*act* mutant, the transposon-induced mutant *V. paradoxus* TBEA6 1/1, and the *V. paradoxus* mutant 1/1 harboring pBBR1MCS-5::$acd_{DPN7}$ were precultivated in liquid MSM containing 50 mM sodium gluconate, supplied with gentamicin if necessary. Prior to inoculation of the main culture, cells were harvested and washed twice with sterile saline. Cultivation was done in liquid MSM containing 50 mM 3SP in Klett flasks with baffles at 30°C and with agitation at 120 rpm. ■, *V. paradoxus* TBEA6 wild type; ▲, *V. paradoxus* TBEA6 Δ*act* mutant; ◆, *V. paradoxus* TBEA6 mutant 1/1; ●, *V. paradoxus* mutant 1/1 harboring pBBR1MCS-5::$acd_{DPN7}$. Bars indicate standard deviations ($n = 3$).

tivated on MSM agar plates containing 20 mM gluconate or 20 mM TDP or 3SP, respectively. While all strains showed growth on gluconate, only *V. paradoxus* strain TBEA6 was able to utilize TDP or 3SP as the sole source of carbon and energy.

**The *V. paradoxus* Δ*act* precise deletion mutant and complementation of the transposon-induced disruption of *act* in *V. paradoxus* mutant 1/1.** The *V. paradoxus* Δ*act* precise deletion mutant was constructed to verify the observed phenotype and to exclude polar effects of the transposon insertion. Surprisingly, the *V. paradoxus* Δ*act* mutant showed normal growth when cultivated on solid MSM plates containing 20 mM TDP or 20 mM 3SP. After complementation with pBBR1MCS-5::$acd_{DPN7}$, harboring the 3SP-CoA desulfinase gene from *A. mimigardefordensis* strain DPN7$^T$ (51), growth of mutant *V. paradoxus* 1/1 was restored on MSM agar plates containing 20 mM 3SP but not on MSM agar plates containing 20 mM TDP. In liquid MSM containing 50 mM 3SP, both the *V. paradoxus* wild type and Δ*act* mutant showed similar growth behaviors (Fig. 3). *V. paradoxus* TBEA6 1/1 showed no growth, while slow but significant growth was observed for the complemented strain *V. paradoxus* TBEA6 1/1(pBBR1MCS-5::$acd_{DPN7}$) under the same conditions. These results indicated a polar effect of the transposon on $acd_{TBEA6}$, located downstream of $act_{TBEA6}$. This 3SP-CoA desulfinase catalyzes the hydrolysis of 3SP-CoA, the potential reaction product of $Act_{TBEA6}$.

**Sequence analyses of $Act_{TBEA6}$.** Sequence analyses showed that the N-terminal part (residues 81 to 270) of $Act_{TBEA6}$ affiliates the enzyme to Pfam02515 (CoA-transferase family III) (see Fig. S2 in the supplemental material). It contains a highly conserved residue (Asp180 in *V. paradoxus* strain TBEA6, Asp169 with respect to CaiB, indicated by an asterisk in Fig. S2) (30), which is located in the active site and binds the organic acid substrate via an anhydride bond (30, 31). Other residues (Arg16, Gly37, Ala38, Val40, Asp90, Leu184, His185, Gly193, and Thr190, referring to CaiB numbering; indicated by ▼ in Fig. S2) (30) are considered to be important for folding, and they are conserved throughout CoA-transferase family III (30). Most of them are found in the same position in $Act_{TBEA6}$ as well. Two minor exceptions are the substitution of a residue corresponding to $Arg16^{CaiB}$ by lysine ($Lys13^{TBEA6}$) in *V. paradoxus* strain TBEA6 and an additional glutamine residue ($Gln196^{TBEA6}$) between $Leu195^{TBEA6}$ (corresponding to $Leu184^{CaiB}$) and $His197^{TBEA6}$ (corresponding to $His185^{CaiB}$).

**Secondary structure analyses.** The amino acid sequences of $Act_{TBEA6}$ and its orthologues were subjected to secondary structure prediction by the Jpred server (44) (see Fig. S2 in the supplemental material). Due to their available solved crystal structures, formyl-CoA:oxalate CoA-transferase from *E. coli* (YfdW) (27, 28), its orthologue Frc from *Oxalobacter formigenes* (20, 26), and crotonobetainyl-CoA:carnitine CoA-transferase from *E. coli* (CaiB) (29, 30) as members of the CoA-transferase III family were included for comparison. As shown in Fig. S2, the amino acid sequences of $Act_{TBEA6}$, $Act_{DPN7}$, and $Act_{LB400}$ (YP_553419.1) are truncated by about 13 to 15 amino acid residues in comparison to all other included sequences.

**Cloning of the putative acyl-CoA-transferase gene $act_{TBEA6}$ into the vector pET22b(+), overexpression in *E. coli* Lemo21(DE3), and purification and characterization of the translational product.** Based on nucleotide sequence data (GenBank accession no. ACC69030.2), native $Act_{TBEA6}$ has a calculated molecular mass of 43.322 kDa (isotopically average), consists of 398 amino acids, and has a calculated pI of 5.46. In this study, the putative *act* gene of *V. paradoxus* strain TBEA6 was heterologously expressed as a $His_6$-tagged protein using the T7-promoter/polymerase-based expression vector pET22b(+) and *E. coli* Lemo21(DE3) as the host strain. For this, the protein was equipped with an additional C-terminal $His_6$ tag plus two vector-encoded amino acids (leucine and glutamate) and an N-terminal *pelB* signal sequence (22 amino acids plus 17 amino acids between *pelB* and the start of *act*) for potential periplasmatic localization (see Materials and Methods) (see Fig. S1 in the supplemental material). Consequently, the heterologously expressed protein consisted of 445 amino acids, and it exhibited a theoretical molecular mass of 48.372 Da (isotopically average) and a theoretical pI of 5.65. The overproduced enzyme was purified by immobilized metal chelate affinity chromatography to electrophoretic homogeneity (Fig. 4). Afterwards, $Act_{TBEA6}$ was applied to analytical size exclusion chromatography. It revealed an apparent molecular mass of 96 ± 3 kDa. This corresponds to a homodimer of the protein with a theoretical molecular mass of 96.7 kDa, including the $His_6$ tag and the additional 39 amino acid residues of the N-terminal *pelB* signal sequence. The UV-visible spectrum (λ = 200

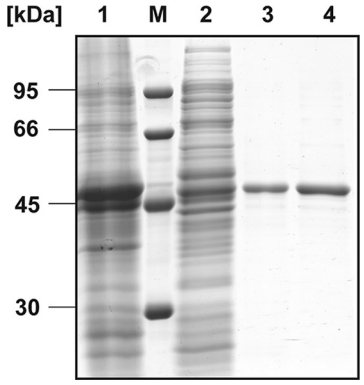


**FIG 4** Purification of $Act_{TBEA6}$ by affinity chromatography as revealed by SDS-PAGE. Lane 1, crude extract of cells; lane M, molecular mass marker; lane 2, soluble fraction after centrifugation; lane 3, elution fraction after Ni-NTA affinity chromatography column; lane 4, pooled fractions recovered after Superdex 200 HR size exclusion chromatography. Forty micrograms of protein was applied in lanes 1 and 2. Lanes 3 and 4 were loaded with 5 μg protein. The SDS gel was stained with Coomassie brilliant blue R.

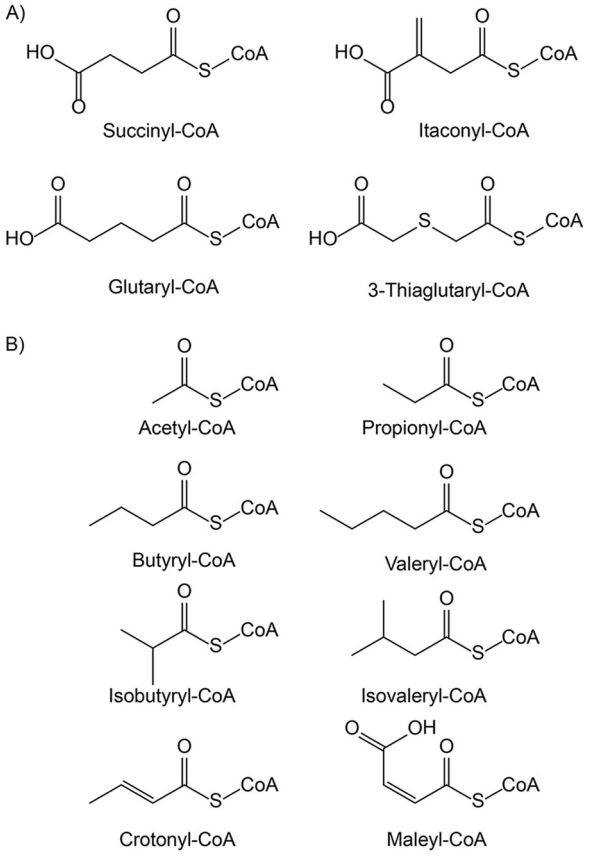


**FIG 5** Structures of acyl-CoA thioesters used in this study. (A) CoA thioesters that were identified as CoA donors of $Act_{TBEA6}$; (B) CoA thioesters that were not accepted as CoA donors by $Act_{TBEA6}$.

to 800 nm) of purified $Act_{TBEA6}$ showed a single peak at 280 nm, which indicates the absence of any chromophoric cofactor.

**Act enzyme activity assays applying the heterologously expressed and purified protein. (i) Initial identification of an appropriate CoA-donor for $Act_{TBEA6}$.** In an early test, acetyl-CoA, propionyl-CoA, butyryl-CoA, crotonyl-CoA, and succinyl-CoA were applied as potential CoA donors of $Act_{TBEA6}$ as described in Materials and Methods. Formation of 3SP-CoA (*m*/*z* 888) was only observed when succinyl-CoA was applied in the assay mixture but not for any of the other CoA esters (data not shown). No 3SP-CoA was detected in negative controls containing heat-inactivated enzyme (15 min at 95°C), applying soluble protein fractions from cells harboring only the expression vector without $act_{TBEA6}$ (vector control) or by omitting one of the substrates at a time.

**(ii) Determination of kinetic parameters.** Only recently, we reported the characterization of $Acd_{DPN7}$, a 3SP-CoA desulfinase from *A. mimigardefordensis* strain DPN7$^T$ (51). The equimolar release of sulfite from 3SP-CoA by $Acd_{DPN7}$ was quantified in a continuous spectrophotometric assay with DTNB, Ellman's reagent, and served to determine the kinetic parameters of $Acd_{DPN7}$. In this study, we applied $Acd_{DPN7}$ as an auxiliary enzyme in a coupled enzyme assay and indirectly monitored the formation of 3SP-CoA by $Act_{TBEA6}$, which resulted in an increase in absorption at 412 nm ($\varepsilon$ = 14.150 $mM^{-1}$ $cm^{-1}$). The apparent $V_{max}$ for succinyl-CoA was 44.6 μmol $min^{-1}$ $mg^{-1}$, which corresponds to a turnover number of 36.0 $s^{-1}$ per subunit of $Act_{TBEA6}$. The apparent $V_{max}$ for 3SP was 46.8 μmol $min^{-1}$ $mg^{-1}$, which corresponds to a turnover number of 37.7 $s^{-1}$ per subunit of $Act_{TBEA6}$. The $K_m$ values were 0.08 mM for succinyl-CoA and 5.9 mM for 3SP (Table 2).

**(iii) Utilization of CoA donors other than succinyl-CoA.** $Act_{TBEA6}$ utilized only CoA thioesters of dicarboxylic acids as CoA donors in the following order: succinyl-CoA ≫ glutaryl-CoA > itaconyl-CoA > 3-thiaglutaryl-CoA (Fig. 5A and 6). Interestingly, maleyl-CoA did not serve as a CoA donor. Furthermore, $Act_{TBEA6}$ was not active with CoA esters of monocarboxylic acids like acetyl-CoA, propionyl-CoA, butyryl-CoA, valeryl-CoA, isobutyryl-CoA, isovaleryl-CoA, or crotonyl-CoA (Fig. 5B).

**(iv) Equilibrium between succinyl-CoA or glutaryl-CoA and 3SP-CoA.** HPLC-ESI-MS analyses indicate that at equilibrium,

**TABLE 2** Kinetic parameters of succinyl-CoA:3-sulfinopropionate CoA-transferase

| Enzyme | Mol mass (subunit), kDa | Subunit composition | Substrate | $V_{max}$ (μmol $min^{-1}$ $mg^{-1}$) | $K_m$ (mM) | $k_{cat}$ ($s^{-1}$) | $k_{cat}/K_m$ ($s^{-1}$ $mM^{-1}$) |
|---|---|---|---|---|---|---|---|
| $Act_{TBEA6}$ | 48.4 | $\alpha_2$ | Succinyl-CoA | 44.6 | 0.08 | 36.0 | 448.5 |
| | | | 3SP | 46.8 | 5.9 | 37.7 | 6.4 |
| $SucCD_{DPN7}$[a] | 72.2[b] | $(\alpha\beta)_2$ | 3SP | 0.12 | 0.818 | 0.1[c] | 0.18[c] |

[a] The $V_{max}$ and $K_m$ for succinyl-CoA synthetase (SucCD) from *A. mimigardefordensis* DPN7$^T$ have been reported previously (37).
[b] Calculation is based on available amino acid sequences of $SucCD_{DPN7}$ subunits (ACB59226.1 and ACB59227.1).
[c] The kinetic parameter has been calculated based on values available from the literature.

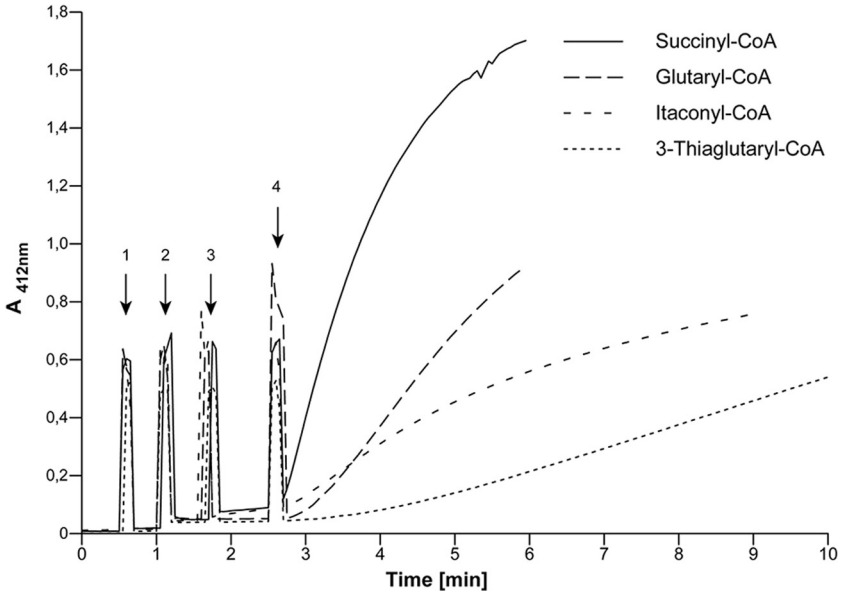


**FIG 6** Identification of putative CoA donors of $Act_{TBEA6}$. The assay mixture contained 0.2 mM DTNB, 10 mM 3SP, and an excess of $Acd_{DPN7}$ in 50 mM Tris-HCl (pH 7.6)–150 mM NaCl in a final volume of 1 ml. CoA thioesters were added to a final concentration of 0.13 mM. Addition of assay components is indicated by arrows: 1, 50 μl 3SP solution; 2, 50 μl solution containing $Acd_{DPN7}$ as an auxiliary enzyme; 3, 10 μl of the respective CoA thioester; 4, 10 μl containing 42 μg of purified $Act_{TBEA6}$. The rise in absorption at the times of addition is due to opening of the spectrophotometer.

more 3SP-CoA is formed than succinyl-CoA (Fig. 7). In contrast to this, the reaction equilibrium favors the side of the educts when glutaryl-CoA was used as a CoA donor.

**(v) Utilization of other CoA acceptors than 3SP.** $Act_{TBEA6}$ can catalyze the CoA transfer from succinyl-CoA to itaconate and glutarate as shown by HPLC-ESI MS analyses. Acetate, propionate, fumarate, and mercaptosuccinate were not appropriate CoA acceptors (data not shown).

**Inactivation experiments with hydroxylamine and sodium borohydride.** Members of the CoA-transferase family I are inactivated by low concentrations of hydroxylamine or sodium borohydride in the presence of an appropriate CoA donor due to their ping-pong mechanism. Enzymes that belong to CoA-transferase family II are subunits within a lyase complex. Members of this family catalyze the reaction via a ternary complex, which renders them insensitive to hydroxylamine or sodium borohydride (21). Results for inhibition experiments with members of CoA-transferase family III applying hydroxylamine and sodium borohydride are ambiguous (20, 55–59). Hence, both compounds were tested for a potential inactivating effect on $Act_{TBEA6}$ (see Materials and Methods). When purified $Act_{TBEA6}$ was preincubated for 10 min in the presence of 2 mM succinyl-CoA and 10 mM hydroxylamine, 75% of the activity was retained. After preincubation with 1 mM $NaBH_4$ in the presence of 2 mM succinyl-CoA, nearly 75% of the activity was retained, and the activity was reduced to 9% when $Act_{TBEA6}$ was preincubated in the presence of 2 mM succinyl-CoA and 10 mM $NaBH_4$.

## DISCUSSION

Bruland et al. (19) observed the accumulation of 3SP as a proposed TDP degradation product during cultivation of a Tn*5*::*mob*-induced *V. paradoxus* TBEA6 mutant in MSM containing TDP. In contrast to the wild type, this mutant was unable to utilize 3SP as the sole source of carbon and energy for growth. The insertion of Tn*5*::*mob* in this mutant was mapped in a gene putatively coding for an acyl-CoA-transferase ($Act_{TBEA6}$) (19). The aim of the present study was to characterize the role of $Act_{TBEA6}$ during TDP degradation.

**Identification of a gene cluster potentially essential for degradation of 3SP.** The gene region upstream of $act_{TBEA6}$ was unknown. As revealed in the present study, the same gene organization in proximity to *act* is found in *V. paradoxus* TBEA6 and in *A. mimigardefordensis* DPN7$^T$ (Fig. 2). This gene cluster is absent in *V. paradoxus* strains S110, EPS, and B4, from which the whole genome sequences are available (53, 60, 61; U. Brandt, S. Hiessl, J. Schuldes, A. Thürmer, J. H. Wübbeler, R. Daniel, and A. Steinbüchel, unpublished data). Furthermore, the latter three strains were unable to utilize TDP or 3SP as sole sources of carbon and energy. *A. mimigardefordensis* strain DPN7$^T$ is a betaproteobacterium that can utilize 3,3′-dithiodipropionate (DTDP), a structural analogue of TDP, and is able to grow on 3SP (9). The catabolic pathway of DTDP has been completely elucidated (37, 51, 62) (Fig. 1). Both strains possess a *lysR-act-acd* gene cluster with high similarity regarding the amino acid sequence of the translation products (*lysR*, 74% identical amino acid residues, 88% similar amino acid residues; *act*, 76% identical and 84% similar; *acd*, 79% identical and 88% similar) (Fig. 2). Only recently, the last step of DTDP degradation in *A. mimigardefordensis* strain DPN7$^T$ has been affiliated to $Acd_{DPN7}$ from the aforementioned gene cluster (51). Interestingly, $Acd_{TBEA6}$ shows high homology to $Acd_{DPN7}$ from *A. mimigardefordensis* strain DPN7$^T$ (79% identical and 88% similar amino acid residues). Hence, it was likely that the degradation of TDP and DTDP occurs, at least in part, via a similar pathway. It might be interesting to investigate, if *B. xenovorans* LB400 can also utilize 3SP as the sole source of carbon and energy.

**Activation of 3SP to 3SP-CoA prior to the final desulfination step.** Activation of 3SP to 3SP-CoA is necessary prior to sulfur abstraction by Acd, as shown in a previous study (51). In the study

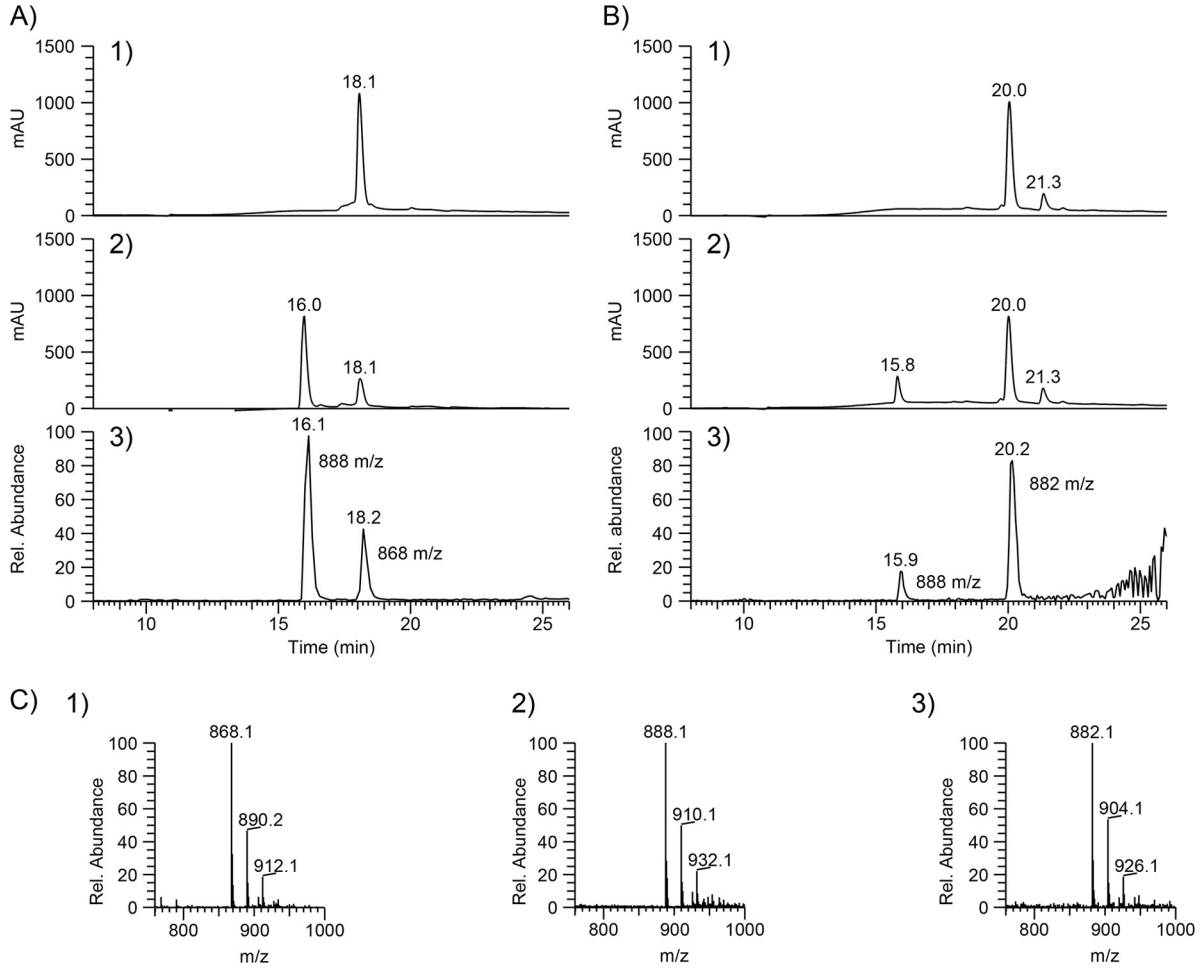


**FIG 7** Formation of 3SP-CoA by $Act_{TBEA6}$ as revealed by HPLC-ESI MS analyses. (A) CoA transfer from succinyl-CoA to 3SP. mAU, milliabsorbance units. (Panel 1) Assay solution containing 0.1 mM succinyl-CoA and 5 mM 3SP in 50 mM Tris-HCl (pH 7.4). (Panel 2) Subsequently, 25 μg of purified $Act_{TBEA6}$ was added and the mixture was incubated for 10 min at 30°C. (Panel 3) ESI MS in the positive mode revealed formation of 3SP-CoA (*m/z* 888) and the presence of the remaining succinyl-CoA (*m/z* 868). (B) CoA transfer from glutaryl-CoA to 3SP. (Panel 1) Assay solution containing 0.1 mM glutaryl-CoA and 5 mM 3SP in 50 mM Tris-HCl (pH 7.4). (Panel 2) Subsequently, of 25 μg of purified $Act_{TBEA6}$ was added, and the mixture was incubated for 10 min at 30°C. (Panel 3) ESI MS in the positive mode revealed formation of 3SP-CoA (*m/z* 888) and the presence of the remaining glutaryl-CoA (*m/z* 882). CoA thioesters were detected at 259 nm. (C) Mass spectra of the respective CoA thioesters. (Panel 1) Succinyl-CoA: retention time (RT), 18.2 in A1; normalization level (NL), 5.65E3. (Panel 2) 3SP-CoA: RT, 16.3 min in A2; NL, 5.67E3. (Panel 3) Glutaryl-CoA: RT, 20.1 min in B2; NL, 1.08E4.

by Bruland et al. (19), the gene $act_{TBEA6}$ was found in close proximity to $acd_{TBEA6}$ and annotated as an acyl-CoA-transferase gene. Hence, we assumed that $Act_{TBEA6}$ might catalyze the activation of 3SP to 3SP-CoA in *V. paradoxus* strain TBEA6, and we investigated the biochemical characteristics of the purified enzyme.

**Biochemical characterization and physiological role of $Act_{TBEA6}$.** First attempts to express $act_{TBEA6}$ in *E. coli* using hybrid plasmids of pET23a(+) and pET19b (Novagen, Madison, WI) resulted in the formation of insoluble protein. Finally, $act_{TBEA6}$ was heterologously expressed in *E. coli* strain Lemo21(DE3) harboring pET22b(+)::$act_{TBEA6}$ (Fig. 4), and the protein was purified to electrophoretic homogeneity. It was not investigated in detail whether the *pelB* leader sequence enabled (partial) secretion into the periplasm or helped enhance the solubility of the heterologously expressed $Act_{TBEA6}$. However, the apparent molecular mass of 96 ± 3 kDa for $Act_{TBEA6}$, as revealed by size exclusion chromatography, corresponds to a homodimer of the protein. Up to now, all solved protein structures have indicated that family III CoA-transferases appear as intertwined dimers (29). Therein, each monomer forms a ring with a hole in the center through which the other monomer is threaded (29). Without crystal structure information, it is not clear if this applies to $Act_{TBEA6}$ as well.

It was an initial task to identify appropriate CoA donors and to verify the formation of 3SP-CoA by $Act_{TBEA6}$. After identification of succinyl-CoA as an active CoA donor and verification of 3SP-CoA formation using HPLC-ESI MS (Fig. 7), kinetic parameters were determined for $Act_{TBEA6}$ in a continuous spectrophotometric enzyme assay with $Acd_{DPN7}$ as an auxiliary enzyme (Table 2). Although both enzymes belong to different enzyme classes, $Act_{TBEA6}$ was compared with $SucCD_{DPN7}$, which catalyzes the activation of 3SP in *A. mimigardefordensis* $DPN7^T$ (Table 2). $SucCD_{DPN7}$ is an $Mg^{2+}$-dependent succinate:CoA ligase that can activate dicarboxylic acids to the corresponding CoA thioesters under consumption of ATP (or GTP) (37). In contrast to this, $Act_{TBEA6}$ as a representative of the acyl-CoA-transferases, conserves the energy of the thioester bond of a CoA donor during

transfer of the CoA moiety to another carboxylic acid. In terms of $k_{cat}$, $Act_{TBEA6}$ showed an about 370-fold-higher catalytic activity in comparison to $SucCD_{DPN7}$ with regard to 3SP. In contrast to this, $Act_{TBEA6}$ shows less affinity toward 3SP than $SucCD_{DPN7}$, as indicated by the about 7-fold-higher $K_m$ value for the sulfur-containing substrate. Nonetheless, the catalytic efficiency of $Act_{TBEA6}$ toward 3SP is higher, as indicated by $k_{cat}/K_m$. Thus, it might depend on the physiological concentration of 3SP or the other substrates in the cells at a given point of time whether $Act_{TBEA6}$ or $SucCD_{DPN7}$ is better suited for the activation of 3SP. Whether SucCD can compensate for the disruption (mutant 1/1) or the deletion (mutant Δ*act*) of Act is discussed further below.

Additional tests showed that $Act_{TBEA6}$ is not completely specific for just one CoA donor. Instead, $Act_{TBEA6}$ accepts succinyl-CoA, itaconyl-CoA, glutaryl-CoA, and 3-thiaglutaryl-CoA, respectively (Fig. 5A and 6). In contrast to this, CoA thioesters of monocarboxylic acids, such as acetyl-CoA or propionyl-CoA, are not accepted as CoA donors (Fig. 5B). This indicated that a second, terminal carboxy group in the acyl moiety is mandatory. The same seems to apply for CoA acceptor molecules as $Act_{TBEA6}$ could activate itaconate and glutarate, respectively, but not acetate or propionate. Interestingly, $Act_{TBEA6}$ was unable to utilize maleyl-CoA as a CoA donor, and fumarate as a potential CoA acceptor was not activated to the corresponding CoA thioester. Hence, both a *cis* and a *trans* double bond appear to prevent catalysis. The impaired rotation of the carboxy group probably results in sterical hindrance or improper binding of the carboxy group in the catalytical center. With regard to side groups in CoA acceptor molecules, the methylene group in itaconate appears to be less impeding than the sulfhydryl group in mercaptosuccinate. This might be due to the fact that thiols are rather acidic and thus are negatively charged, which might interfere with a proper reaction.

Concerning a potential physiological function, $Act_{TBEA6}$ showed the highest activity with succinyl-CoA (Fig. 6), which is thus expected to be the physiological CoA donor. The ability to activate glutarate to glutaryl-CoA might indicate that $Act_{TBEA6}$ can act as an succinyl-CoA:glutarate CoA-transferase. The enzyme assay that was utilized was based on the formation of 3SP-CoA, which was then cleaved to sulfite and propionyl-CoA by $Acd_{DPN7}$ as an auxiliary enzyme. Hence, the exchange of 3SP and determination of $K_m$ values for other potential CoA acceptors was not possible. Consequently, we could not identify the physiological CoA acceptor of $Act_{TBEA6}$. The ability of $Act_{TBEA6}$ to activate 3SP to 3SP-CoA is most likely due to the structural similarities of succinyl-CoA and 3SP-CoA or succinate and 3SP, respectively. In the latter, a carboxyl group is exchanged by a sulfino group, which is essentially an exchange of a carbon atom by a sulfur atom. Thus, all four of them are recognized by $Act_{TBEA6}$. RT-PCR analyses in the previous study (19) revealed the constitutive transcription of the gene in the wild type, irrespective of whether *V. paradoxus* strain TBEA6 was grown in the presence of TDP or succinate. Nonetheless, the inactivation of $Act_{TBEA6}$ in mutant 1/1 did not affect growth on other carbon sources (19). This indicates that $Act_{TBEA6}$ is not essential for growth or that other enzymes can compensate for inactivated $Act_{TBEA6}$. Thus, the physiological role of $Act_{TBEA6}$ in the absence of TDP or 3SP remains to be elucidated.

**Multiple sequence alignments and comparison with orthologues of $Act_{TBEA6}$.** A BLAST search affiliated the N-terminal part (residues 80 to 270) of the $act_{TBEA6}$ translation product to Pfam02515 (CoA-transferase family III). Additionally, the presence of amino acid residues considered to be involved in folding and therefore expected to be highly conserved throughout CoA-transferase family III allocated $Act_{TBEA6}$ to this class of CoA-transferases (see Fig. S1 in the supplemental material).

The first characterized member of family III is a formyl-CoA:oxalate CoA-transferase (Frc) from *O. formigenes*, which catalyzes the transfer of a CoA moiety between formyl-CoA and oxalate (20, 21, 26, 63, 64). Other enzymes, such as a crotonobetainyl-CoA:L-carnitine CoA-transferase (CaiB) from *E. coli* (29, 30) or succinyl-CoA:(*R*)-benzylsuccinate CoA-transferase from *Thauera aromatica* (57), have been discovered and have been assigned to family III as well. An acyl-CoA:carboxylate CoA-transferase from *Aspergillus nidulans* was characterized as the first eukaryotic member of this enzyme family (65).

Nonetheless, other authors recommended to best describe the structure of its members in terms of α-helices and β-sheets due to the low number of conserved amino acid residues in CoA-transferase family III (26). Frc and CaiB show an N-terminal βαβ motif, which resembles a Rossmann fold and is involved in CoA binding (26). This motif can be found in $Act_{TBEA6}$ and all other compared sequences (see Fig. S2 in the supplemental material).

Hitherto, all investigated CoA-transferases displayed a C-terminal motif of two consecutive α-helices (26–30). The prediction of secondary structures for $Act_{TBEA6}$ and comparison with several orthologues revealed a truncated amino acid sequence resulting in the absence of one of the C-terminal α-helices (see Fig. S2 in the supplemental material). This absence is also observed in closely related Acts, e.g., from *A. mimigardefordensis* strain $DPN7^T$ and *B. xenovorans* strain LB400. Whether this truncation has any effect on catalysis or the substrate spectrum remains to be investigated.

Formation of a ternary complex during catalysis has been proposed for members of the CoA-transferase family III (57). Only recently, the formation of an acid anhydride between an aspartate residue and CoA-activated acid has been verified (20). Consequently, this anhydride intermediate should react with sodium borohydride and hydroxylamine, which inactivates the CoA-transferase permanently. Nonetheless, ambiguous results were obtained regarding sensitivity toward these inhibitors (20, 55–59). $Act_{TBEA6}$ was only partially inactivated by hydroxylamine and sodium borohydride. However, sodium borohydride had a stronger effect (9% remaining activity) than hydroxylamine (75% remaining activity). Two different mechanisms, which close the active site during catalysis, were discovered in members of the family III CoA-transferases. It had been proposed earlier that closure of the active site prevents entry of inhibitor molecules (66). A glycine-rich loop, found in formyl-CoA transferases, caps the active site if the ligand is bound (20, 26, 28). The glycine-rich loop is not conserved among family III CoA-transferases, but a second mechanism was identified in CaiB from *E. coli*. Therein, an induced domain movement could be observed upon binding of CoA, which results in closure of the active site and thereby in protection of the intermediate (30). In Fig. S3 in the supplemental material, the glycine-rich loop is highlighted for formyl-CoA:oxalate CoA-transferase from *E. coli* K-12 substrain MG1655 (AAC75433.1) and from *O. formigenes* (AAC45298.1). $Act_{TBEA6}$ and all other aligned sequences show no such motif, and about 20 to 30 amino acid residues are missing upstream of the glycine-rich loop (see Fig. S3). Since such a glycine-rich loop is missing, the second mechanism appears to be more likely for $Act_{TBEA6}$. The ability to properly close the active site might be responsible for the diverse

sensitivities toward $NaBH_4$ and hydroxylamine of different members of the CoA-transferase family III.

**Compensation of Act activity in *V. paradoxus* TBEA6 Δ*act*.** After biochemical characterization of $Act_{TBEA6}$, deletion of $act_{TBEA6}$ in the *V. paradoxus* Δ*act* defined deletion mutant did not verify the phenotype of the transposon mutant *V. paradoxus* 1/1 from the previous study. Interestingly, growth of *V. paradoxus* mutant 1/1 with 3SP was partially restored by complementation with pBBR1MCS-5::$acd_{DPN7}$ (Fig. 3). This indicated a polar effect of the Tn*5*::*mob* transposon insertion on $acd_{TBEA6}$. The translation product of $acd_{TBEA6}$, located downstream of $act_{TBEA6}$, shows homology to a 3SP-CoA desulfinase in *A. mimigardefordensis* strain $DPN7^T$, which we identified and characterized only recently (51). This enzyme is responsible for the final step during degradation of DTDP. The desulfinase catalyzes the hydrolysis of 3SP-CoA to sulfite and propionyl-CoA, which enters the central metabolism via the methylcitric acid cycle (51). In this study, pBBR1MCS-5::$acd_{DPN7}$ was applied for complementation of an *A. mimigardefordensis* Δ*acd* mutant. Similarly to the present study, growth could be partially restored with 3SP, but not with the precursor DTDP. It was proposed that this is due to low transcription of $Acd_{DPN7}$ and concomitant accumulation of toxic 3MP after cleavage of DTDP, which inhibits growth of the cells (51). 3SP was shown to be nontoxic to cells of *A. mimigardefordensis* $DPN7^T$ when supplied as the sole carbon source in liquid MSM in concentrations of up to 100 mM (C. Meinert, personal communication). Hence, cells of *A. mimigardefordensis* $DPN7^T$ were expected to have enough time to form a sufficient amount of $Acd_{DPN7}$ for growth in the presence of 3SP (51). Further explanations for the lack to fully restore growth in comparison to the wild type might be that a heterologous gene was used or that the ribosomal binding site was not properly recognized.

Moreover, we could confirm desulfination of 3SP-CoA by $Acd_{TBEA6}$ in enzyme assays applying heterologously expressed and purified enzyme (M. Schürmann, R. Demming, M. Krewing, J. Rose, J. H. Wübbeler, and A. Steinbüchel, unpublished results). Hence, a polar effect of the transposon on $Acd_{TBEA6}$ would impair the final step during TDP degradation (Fig. 1 and 2).

However, $act_{TBEA6}$ was disrupted or precisely deleted, respectively, in *V. paradoxus* mutant 1/1 and the *V. paradoxus* Δ*act* strain. Consequently, the necessary activation of 3SP to the corresponding CoA thioester prior to sulfur abstraction by $Acd_{TBEA6}$ has to be compensated for by other enzymes. In *A. mimigardefordensis*, a succinate-CoA ligase (SucCD) from the citric acid cycle catalyzes this reaction (37) (Fig. 1). Furthermore, only recently SucCDs from *E. coli* BL21 (accession no.: α-subunit, YP_002998521.1; β-subunit, YP_002998520.1) and *Alcanivorax borkumensis* (α-subunit, YP_693212.1; β-subunit, YP_693213.1) were investigated with regard to their substrate range in our laboratory (J. Nolte, M. Schürmann, C. L. Schepers, E. Vogel, J. H. Wübbeler, and A. Steinbüchel, unpublished results). Both enzymes accepted 3SP as a substrate with activities comparable to $SucCD_{DPN7}$ reported earlier (67). Hence, we expect this to be a common feature of SucCDs due to the high structural similarity between 3SP and succinate, a physiological substrate of SucCDs in the citric acid cycle. Other strains of *V. paradoxus* like EPS (53) (GenBank accession no. of complete genome, CP002417.1) and S110 (61) (GenBank accession no. CP001635.1 and CP001636.1) possess two SucCD homologues. Therefore, it is likely that *V. paradoxus* strain TBEA6 also possesses two SucCD homologues, and we expect them to catalyze the activation of 3SP to 3SP-CoA. Unfortunately, the whole genome sequence of *V. paradoxus* TBEA6 is unknown, and therefore predictions about structure-substrate specificity relationships as well as precise deletion of both SucCDs are not possible at the moment.

**Conclusions.** In summary, the activation of 3SP to the corresponding CoA thioester by $Act_{TBEA6}$ was clearly shown in this study. Therefore, the systematic name of this novel member of the CoA-transferase family III is "succinyl-CoA:3-sulfinopropionate CoA-transferase." Succinyl-CoA and glutaryl-CoA were identified as potential physiological CoA donors for $Act_{TBEA6}$. Further studies, which will unravel why deletion of $act_{TBEA6}$ can be compensated for in *V. paradoxus* TBEA6, are in progress. Furthermore, it might be interesting to investigate if the *lysR-act-acd* gene cluster can transfer the capability of 3SP degradation to other bacteria and how the cluster is regulated during 3SP degradation in more detail.

## ACKNOWLEDGMENTS

The LC-MS device used in this study was provided by funds of the DFG (Deutsche Forschungsgemeinschaft, grant no. INST 211/415-1 FUGG), which we gratefully acknowledge.

Furthermore, we thank Jong-In Han and Paul Orwin for kindly providing *V. paradoxus* strain S110 and *V. paradoxus* strain EPS, respectively. Moreover, we sincerely thank Christina Doberstein for assistance in literature research.

## REFERENCES

1. **Garde JA, Catala R, Gavara R.** 1998. Global and specific migration of antioxidants from polypropylene films into food simulants. J. Food Prot. **61:**1000–1006.
2. **Scott G.** 1968. Mechanisms of antioxidant action: esters of thiodipropionic acid. Chem. Commun. (Camb.) **24:**1572–1574.
3. **Kúdelka I, Misro PK, Pospíšil J, Korbanka H, Riedel T, Pfahler G.** 1985. Antioxidants and stabilizers. Part IC. Hydroperoxide deactivation by aliphatic sulfides. A model study. Polym. Degrad. Stab. **12:**303–313.
4. **Fehling E, Klein E, Vosmann K, Bergander K, Weber N.** 2008. Linear copolymeric poly(thia-alkanedioates) by lipase-catalyzed esterification and transesterification of 3,3′-thiodipropionic acid and its dimethyl ester with α,ω-alkanediols. Biotechnol. Bioeng. **99:**1074–1084.
5. **Lütke-Eversloh T, Bergander K, Luftmann H, Steinbüchel A.** 2001. Identification of a new class of biopolymer: bacterial synthesis of a sulfur-containing polymer with thioester linkages. Microbiology **147:**11–19.
6. **Lütke-Eversloh T, Bergander K, Luftmann H, Steinbüchel A.** 2001. Biosynthesis of poly(3-hydroxybutyrate-*co*-3-mercaptobutyrate) as a sulfur analogue to poly(3-hydroxybutyrate) (PHB). Biomacromolecules **2:**1061–1065.
7. **Thakor N, Lütke-Eversloh T, Steinbüchel A.** 2005. Application of the BPEC pathway for large-scale biotechnological production of poly(3-mercaptopropionate) by recombinant *Escherichia coli*, including a novel in situ isolation method. Appl. Environ. Microbiol. **71:**835–841.
8. **Lütke-Eversloh T, Steinbüchel A.** 2004. Microbial polythioesters. Macromol. Biosci. **4:**165–174.
9. **Wübbeler JH, Lutke-Eversloh T, Van Trappen S, Vandamme P, Steinbüchel A.** 2006. *Tetrathiobacter mimigardefordensis* sp. nov., isolated from compost, a betaproteobacterium capable of utilizing the organic disulfide 3,3′-dithiodipropionic acid. Int. J. Syst. Evol. Microbiol. **56:**1305–1310.
10. **Xia Y, Wübbeler JH, Qi Q, Steinbüchel A.** 2012. Employing a recombinant strain of *Advenella mimigardefordensis* for biotechnical production of homopolythioesters from 3,3′-dithiodipropionic acid. Appl. Environ. Microbiol. **78:**3286–3297.
11. **Aragno M, Walther-Mauruschat A, Mayer F, Schlegel HG.** 1977. Micromorphology of gram-negative hydrogen bacteria. I. Cell morphology and flagellation. Arch. Microbiol. **114:**93–100.
12. **Willems A, De Ley J, Gillis M, Kersters K.** 1991. *Comamonadaceae*, a new family encompassing the acidovorans rRNA complex, including *Variovorax paradoxus* gen. nov., comb. nov., for *Alcaligenes paradoxus*. Int. J. Syst. Bacteriol. **41:**445–450.

13. **Belimov AA, Safronova VI, Sergeyeva TA, Egorova TN, Matveyeva VA, Tsyganov VE, Borisov AY, Tikhonovich IA, Kluge C, Preisfeld A, Dietz KJ, Stepanok VV.** 2001. Characterization of plant growth promoting rhizobacteria isolated from polluted soils and containing 1-aminocyclopropane-1-carboxylate deaminase. Can. J. Microbiol. **47:**642–652.
14. **Belimov AA, Hontzeas N, Safronova VI, Demchinskaya SV, Piluzza G, Bullitta S, Glick BR.** 2005. Cadmium-tolerant plant growth-promoting bacteria associated with the roots of Indian mustard (*Brassica juncea* L. Czern.). Soil Biol. Biochem. **37:**241–250.
15. **McInroy JA, Kloepper JW.** 1995. Survey of indigenous bacterial endophytes from cotton and sweet corn. Plant Soil **173:**337–342.
16. **Uroz S, D'Angelo-Picard C, Carlier A, Elasri M, Sicot C, Petit A, Oger P, Faure D, Dessaux Y.** 2003. Novel bacteria degrading N-acylhomoserine lactones and their use as quenchers of quorum-sensing-regulated functions of plant-pathogenic bacteria. Microbiology **149:**1981–1989.
17. **Don RH, Weightman AJ, Knackmuss HJ, Timmis KN.** 1985. Transposon mutagenesis and cloning analysis of the pathways for degradation of 2,4-dichlorophenoxyacetic acid and 3-chlorobenzoate in *Alcaligenes eutrophus* JMP134(pJP4). J. Bacteriol. **161:**85–90.
18. **Snellinx Z, Taghavi S, Vangronsveld J, Van der Lelie D.** 2003. Microbial consortia that degrade 2,4-DNT by interspecies metabolism: isolation and characterisation. Biodegradation **14:**19–29.
19. **Bruland N, Wübbeler JH, Steinbüchel A.** 2009. 3-Mercaptopropionate dioxygenase, a cysteine dioxygenase homologue, catalyzes the initial step of 3-mercaptopropionate catabolism in the 3,3-thiodipropionic acid-degrading bacterium *Variovorax paradoxus*. J. Biol. Chem. **284:**660–672.
20. **Berthold CL, Toyota CG, Richards NGJ, Lindqvist Y.** 2008. Reinvestigation of the catalytic mechanism of formyl-CoA transferase, a class III CoA-transferase. J. Biol. Chem. **283:**6519–6529.
21. **Heider J.** 2001. A new family of CoA-transferases. FEBS Lett. **509:**345–349.
22. **Selmer T, Buckel W.** 1999. Oxygen exchange between acetate and the catalytic glutamate residue in glutaconate CoA-transferase from *Acidaminococcus fermentans*. Implications for the mechanism of CoA-ester hydrolysis. J. Biol. Chem. **274:**20772–20778.
23. **Buckel W, Buschmeier V, Eggerer H.** 1971. The action mechanism of citrate lyase from *Klebsiella aerogenes*. Hoppe-Seylers Z. Physiol. Chem. **352:**1195–1205.
24. **Buckel W, Bobi A.** 1976. The enzyme complex citramalate lyase from *Clostridium tetanomorphum*. Eur. J. Biochem. **64:**255–262.
25. **Dimroth P, Eggerer H.** 1975. Evaluation of the protein components of citrate lyase from *Klebsiella aerogenes*. Eur. J. Biochem. **53:**227–235.
26. **Ricagno S, Jonsson S, Richards N, Lindqvist Y.** 2003. Formyl-CoA transferase encloses the CoA binding site at the interface of an interlocked dimer. EMBO J. **22:**3210–3219.
27. **Gogos A, Gorman J, Shapiro L.** 2004. Structure of *Escherichia coli* YfdW, a type III CoA transferase. Acta Crystallogr. D Biol. Crystallogr. **60:**507–511.
28. **Gruez A, Roig-Zamboni V, Valencia C, Campanacci V, Cambillau C.** 2003. The crystal structure of the *Escherichia coli* YfdW gene product reveals a new fold of two interlaced rings identifying a wide family of CoA transferases. J. Biol. Chem. **278:**34582–34586.
29. **Rangarajan ES, Li Y, Iannuzzi P, Cygler M, Matte A.** 2005. Crystal structure of *Escherichia coli* crotonobetainyl-CoA: carnitine CoA-transferase (CaiB) and its complexes with CoA and carnitinyl-CoA. Biochemistry **44:**5728–5738.
30. **Stenmark P, Gurmu D, Nordlund P.** 2004. Crystal structure of CaiB, a type-III CoA transferase in carnitine metabolism. Biochemistry **43:**13996–14003.
31. **Jonsson S, Ricagno S, Lindqvist Y, Richards NGJ.** 2004. Kinetic and mechanistic characterization of the formyl-CoA transferase from *Oxalobacter formigenes*. J. Biol. Chem. **279:**36003–36012.
32. **Schlegel HG, Kaltwasser H, Gottschalk G.** 1961. A submersion method for culture of hydrogen-oxidizing bacteria: growth physiological studies. Arch. Mikrobiol. **38:**209–222.
33. **Sambrook J, Fritsch EF, Maniatis T.** 1989. Molecular cloning: a laboratory manual, 2nd ed. Cold Spring Harbor Laboratory Press, Cold Spring Harbor, NY.
34. **Studier FW.** 2005. Protein production by auto-induction in high density shaking cultures. Protein Expr. Purif. **41:**207–234.
35. **Jolles-Bergeret B.** 1974. Enzymatic and chemical synthesis of 3-sulfinopropionic acid, an analog of succinic acid. Eur. J. Biochem. **42:**349–353.
36. **Wübbeler JH, Bruland N, Kretschmer K, Steinbüchel A.** 2008. Novel pathway for catabolism of the organic sulfur compound 3,3′-dithiodipropionic acid via 3-mercaptopropionic acid and 3-sulfinopropionic acid to propionyl-coenzyme A by the aerobic bacterium *Tetrathiobacter mimigardefordensis* strain DPN7. Appl. Environ. Microbiol. **74:**4028–4035.
37. **Schürmann M, Wübbeler JH, Grote J, Steinbüchel A.** 2011. Novel reaction of succinyl coenzyme A (succinyl-CoA) synthetase: activation of 3-sulfinopropionate to 3-sulfinopropionyl-CoA in *Advenella mimigardefordensis* strain DPN7$^T$ during degradation of 3,3′-dithiodipropionic acid. J. Bacteriol. **193:**3078–3089.
38. **Simon EJ, Shemin D.** 1953. The preparation of S-succinyl coenzyme A. J. Am. Chem. Soc. **75:**2520.
39. **Ellman GL.** 1959. Tissue sulfhydryl groups. Arch. Biochem. Biophys. **82:**70–77.
40. **Marmur J.** 1961. A procedure for isolation of deoxyribonucleic acid from microorganism. J. Mol. Biol. **3:**208–218.
41. **Sanger F, Coulson AR, Hong GF, Hill DF, Petersen GB.** 1982. Nucleotide sequence of bacteriophage λ DNA. J. Mol. Biol. **162:**729–773.
42. **Altschul SF, Madden TL, Schaffer AA, Zhang J, Zhang Z, Miller W, Lipman DJ.** 1997. Gapped BLAST and PSI-BLAST: a new generation of protein database search programs. Nucleic Acids Res. **25:**3389–3402.
43. **Hall T.** 1999. BioEdit: a user-friendly biological sequence alignment editor and analysis program for Windows 95/98/NT. Nucleic Acids Symp. Ser. (Oxf.) **41:**95–98.
44. **Cole C, Barber JD, Barton GJ.** 2008. The Jpred 3 secondary structure prediction server. Nucleic Acids Res. **36:**W197–W201.
45. **Gasteiger E, Gattiker A, Hoogland C, Ivanyi I, Appel RD, Bairoch A.** 2003. ExPASy: the proteomics server for in-depth protein knowledge and analysis. Nucleic Acids Res. **31:**3784–3788.
46. **Pilhofer M, Bauer AP, Schrallhammer M, Richter L, Ludwig W, K-, Schleifer Petroni G.** 2007. Characterization of bacterial operons consisting of two tubulins and a kinesin-like gene by the novel two-step gene walking method. Nucleic Acids Res. **35:**e135. doi:10.1093/nar/gkm836.
47. **Pötter M, Müller H, Steinbüchel A.** 2005. Influence of homologous phasins (PhaP) on PHA accumulation and regulation of their expression by the transcriptional repressor PhaR in Ralstonia eutropha H16. Microbiology **151:**825–833.
48. **Simon R, Priefer U, Puhler A.** 1983. A broad host range mobilization system for in vivo genetic engineering: transposon mutagenesis in gram negative bacteria. Biotechnology (NY) **1:**784–791.
49. **Quandt J, Hynes MF.** 1993. Versatile suicide vectors which allow direct selection for gene replacement in Gram-negative bacteria. Gene **127:**15–21.
50. **Friedrich B, Hogrefe C, Schlegel HG.** 1981. Naturally occurring genetic transfer of hydrogen-oxidizing ability between strains of *Alcaligenes eutrophus*. J. Bacteriol. **147:**198–205.
51. **Schürmann M, Deters A, Wübbeler JH, Steinbüchel A.** 2013. A novel 3-sulfinopropionyl coenzyme A (3SP-CoA) desulfinase from *Advenella mimigardefordensis* strain DPN7$^T$ acting as a key enzyme during catabolism of 3,3′-dithiodipropionic acid is a member of the acyl-CoA dehydrogenase superfamily. J. Bacteriol. **195:**1538–1551.
52. **Kovach ME, Elzer PH, Hill DS, Robertson GT, Farris MA, Roop RM, Peterson KM.** 1995. Four new derivatives of the broad-host-range cloning vector pBBR1MCS, carrying different antibiotic-resistance cassettes. Gene **166:**175–176.
53. **Jamieson WD, Pehl MJ, Gregory GA, Orwin PM.** 2009. Coordinated surface activities in *Variovorax paradoxus*. EPS. BMC Microbiol. **9:**124. doi:10.1186/1471-2180-9-124.
54. **Dalluge JJ, Gort S, Hobson R, Selifonova O, Amore F, Gokarn R.** 2002. Separation and identification of organic acid-coenzyme A thioesters using liquid chromatography/electrospray ionization-mass spectrometry. Anal. Bioanal. Chem. **374:**835–840.
55. **Friedmann S, Alber BE, Fuchs G.** 2006. Properties of succinyl-coenzyme A:D-citramalate coenzyme A transferase and its role in the autotrophic 3-hydroxypropionate cycle of *Chloroflexus aurantiacus*. J. Bacteriol. **188:**6460–6468.
56. **Friedmann S, Steindorf A, Alber BE, Fuchs G.** 2006. Properties of succinyl-coenzyme A:L-malate coenzyme A transferase and its role in the autotrophic 3-hydroxypropionate cycle of *Chloroflexus aurantiacus*. J. Bacteriol. **188:**2646–2655.
57. **Leutwein C, Heider J.** 2002. (*R*)-Benzylsuccinyl-CoA dehydrogenase of

*Thauera aromatica*, an enzyme of the anaerobic toluene catabolic pathway. Arch. Microbiol. **178:**517–524.
58. **Dickert S, Pierik AJ, Linder D, Buckel W.** 2000. The involvement of coenzyme A esters in the dehydration of (*R*)-phenyllactate to (*E*)-cinnamate by *Clostridium sporogenes*. Eur. Biochem. **267:**3874–3884.
59. **Kim J, Darley D, Selmer T, Buckel W.** 2006. Characterization of (*R*)-2-hydroxyisocaproate dehydrogenase and a family III coenzyme A transferase involved in reduction of L-leucine to isocaproate by *Clostridium difficile*. Appl. viron. Microbiol. **72:**6062–6069.
60. **Carbajal-Rodriguez I, Stoveken N, Satola B, Wübbeler JH, Steinbüchel A.** 2011. Aerobic degradation of mercaptosuccinate by the Gram-negative bacterium *Variovorax paradoxus* strain B4. J. cteriol. **193:**527–539.
61. **Han JI, Choi HK, Lee SW, Orwin PM, Kim J, Laroe SL, Kim TG, O'Neil J, Leadbetter JR, Lee SY, Hur CG, Spain JC, Ovchinnikova G, Goodwin L, Han C.** 2011. Complete genome sequence of the metabolically versatile plant growth-promoting endophyte *Variovorax paradoxus* S110. J. cteriol. **193:**1183–1190.
62. **Wübbeler JH, Raberg M, Brandt U, Steinbüchel A.** 2010. Dihydrolipoamide dehydrogenases of *Advenella mimigardefordensis* and *Ralstonia eutropha* catalyze cleavage of 3,3′-dithiodipropionic acid into 3-mercaptopropionic acid. Appl. Environ. Microbiol. **76:**7023–7028.
63. **Baetz AL, Allison MJ.** 1990. Purification and characterization of formylcoenzyme A transferase from *Oxalobacter formigenes*. J. Bacteriol. **172:**3537–3540.
64. **Sidhu H, Ogden SD, Lung H-Y, Luttge BG, Baetz AL, Peck AB.** 1997. DNA sequencing and expression of the formyl coenzyme A transferase gene, *frc*, from *Oxalobacter formigenes*. J. Bacteriol. **179:**3378–3381.
65. **Fleck CB, Brock M.** 2008. Characterization of an acyl-CoA:carboxylate CoA-transferase from *Aspergillus nidulans* involved in propionyl-CoA detoxification. Mol. Microbiol. **68:**642–656.
66. **Zarzycki J, Brecht V, Müller M, Fuchs G.** 2009. Identifying the missing steps of the autotrophic 3-hydroxypropionate $CO_2$ fixation cycle in *Chloroflexus aurantiacus*. Proc. Natl. Acad. Sci. U. S. A. **106:**21317–21322.
67. **Bachmann BJ.** 1990. Linkage map of Escherichia coli K-12, ed 8. Microbiol. Rev. **54:**130–197.